A 3-Step Pretargeting Strategy to Image Infection

Otto C. Boerman, Julliette van Eerd, Wim J.G. Oyen, and Frans H.M. Corstens

Department of Nuclear Medicine, University Hospital Nijmegen, Nijmegen, The Netherlands

A new 3-step approach to imaging infectious and inflammatory foci was developed and optimized in a rat model. The approach relies on the nonspecific localization of an anti-diethylenetri-aminepentaacetic acid (DTPA) antibody in inflamed tissue. In this study, the 3-step strategy was optimized by selecting the most suitable radiolabeled hapten and tuning the dosing schedule. **Methods:** Wistar rats with *Staphylococcus aureus* infection in the left calf muscle were primed with the anti-DTPA antibody DTIn-1 (0.67, 2, or 6 nmol per rat). In the second step (1–24 h later), the anti-DTPA activity in the circulation was blocked with unlabeled bovine serum albumin DTPA-In (0.3, 1, or 3 nmol per rat). In the third step (5–30 min later), the radiolabeled hapten (monovalent or bivalent ^{111}In-DTPA) was administered. The in vivo distribution of the radiolabel was monitored by scintigraphic imaging and by ex vivo counting of dissected tissues. **Results:** Scatchard analysis revealed that the affinity of DTIn-1 for bivalent DTPA-^{111}In (^{111}In-diDTPA) was 6 times higher than the affinity for monovalent ^{111}In-DTPA ($K_a = 0.87 \times 10^{-9}$ mol/L vs. 5.3×10^{-9} mol/L). The uptake of the bivalent chelate in the abscess was 2.5-fold higher than that of monovalent ^{111}In-DTPA. Most important, the bivalent chelate was completely retained in the abscess over time. Using the bivalent chelate, the optimal dosing scheme was determined with respect to the DTIn-1 dose (2 nmol per rat), the blocking agent dose (1 nmol per rat), and radiolabeled chelate dose (40 pmol per rat). The procedure was rapid; the infectious focus was clearly visualized 1 h after injection of the ^{111}In-labeled diDTPA, which was 5 h after administration of the anti-DTPA antibody. The nontargeted radiolabel rapidly cleared to the urine, only being retained in the abscess and the kidneys (4–6 percentage injected dose). Finally, an N_2S_2 core was attached to the diDTPA compound, allowing the use of ^{99m}Tc. **Conclusion:** This 3-step approach enables rapid imaging of infectious foci with minimal uptake in noninflamed tissues.

Key Words: pretargeting; infection imaging; bivalent hapten; anti-DTPA antibody

J Nucl Med 2001; 42:1405–1411

Accurate and timely detection of the localization of infection and inflammation may have important implications for the management of patients with infectious or inflammatory diseases. A large series of radiopharmaceuticals has been proposed for scintigraphic imaging of infec-

tion and inflammation. However, limitations inherent to these agents warrant the search for an agent that can be prepared off the shelf and that enables rapid and accurate visualization of inflammatory foci throughout the body.

In radioimmunodetection and radioimmunotherapy of tumors, the targeting of the radiolabel to the tumor could be improved with a pretargeting strategy (*1*). In such a pretargeting approach, an unlabeled antibody is administered in the first step. This antibody localizes in the target tissue, and the target is pretargeted. After the antibody activity has been removed from the circulation, a radiolabeled hapten with affinity for the targeted antibody is administered as a low-molecular-weight ligand. Studies in animal models and in human patients have shown that pretargeting not only can improve target-to-nontarget ratios but also can shorten the imaging procedure (*2–5*). In a previous study, we showed the feasibility of a pretargeting approach for the scintigraphic detection of infection. In that study in rats with focal *Staphylococcus aureus* infection, ^{99m}Tc-diethylenetriamine-pentaacetic acid (DTPA) was trapped in the infection by the preinjected anti-DTPA monoclonal antibody DTIn-1 (*6*). Infectious foci could be visualized by priming the animals with anti-DTPA monoclonal antibody. Four hours later, the circulating anti-DTPA activity was blocked by injecting albumin substituted with DTPA. A fraction of the subsequently administered ^{99m}Tc-DTPA was trapped rapidly in the infected tissue, whereas the nontargeted ^{99m}Tc-DTPA cleared rapidly through the kidneys. In this study, this approach was further optimized by selecting the most suitable radiolabeled hapten and tuning the dosing schedule.

MATERIALS AND METHODS

Monoclonal Antibody

The production of anti-DTPA monoclonal antibody DTIn-1 (IgG2a) has been described (*7*). The antibody binds to DTPA loaded with various trivalent metals, such as chromium, zinc, iron, yttrium, and indium. The antibody was isolated from concentrated hybridoma culture medium (Integra CL350 culture flask; Integra Biosciences, Wallisellen, Switzerland) by protein-A affinity chromatography (*7*).

Blocking Agents

Bovine serum albumin (BSA) (Sigma Chemical, St. Louis, MO) was conjugated with the cyclic anhydride of DTPA (cDTPA) (Sigma Chemical), as described by Hnatowich et al. (*8*). A 100-fold molar excess of cDTPA was added to BSA (10 mg/mL) in 0.1 mol/L NaHCO$_3$ buffer (pH 8.2) and was incubated for 30 min. Approximately 7 DTPA moieties were conjugated per BSA mol-

ecule. Nonconjugated DTPA was removed by extensive dialysis against metal-free 0.1 mol/L citrate buffer (pH 5.0), and the DTPA moieties were loaded with nonradioactive In^{3+} by adding a 3-fold molar excess of $InCl_3$ (Merck, Darmstadt, Germany). Similarly, IgM (ICN, Costa Mesa, CA) was conjugated with cDTPA; cDTPA was added (0.45 mg/mg of IgM) to a solution of IgM (10 mg/mL) in 0.1 mol/L $NaHCO_3$.

Radiolabeled Compounds

[111]In-labeled human IgG was used as a reference in these studies. Polyclonal human nonspecific IgG (Baxter, Lessines, Belgium) was conjugated with cDTPA and labeled with [111]In (7). The radiochemical purity was determined by instant thin-layer chromatography (ITLC) on silica strips (Gelman Sciences, Ann Arbor, MI) using 0.15 mol/L citrate buffer (pH 6.0) as the mobile phase.

[111]In-labeled DTPA was prepared by adding 85 μL [111]$InCl_3$ (Mallinckrodt, Petten, The Netherlands) to 150 μL 0.5 mol/L sodium citrate (pH 4.0) and 10 μL DTPA (5.3×10^{-5} mol/L in 0.5 mol/L sodium acetate, pH 4.0) and incubated for 60 min at room temperature. Complexing of ^{111}In was assessed by ITLC on silica gel strips (Gelman Sciences) with methanol:water (55:45) as the mobile phase. The preparations were checked for the presence of colloid by ITLC using 0.15 mol/L citrate (pH 6.0) as the mobile phase. Nonradioactive In-DTPA was prepared similarly: 10 μL $InCl_3$ (4.19×10^{-4} mol/L in 40 mmol/L HCl), 50 μL 0.5 mol/L sodium citrate (pH 4.0), and 500 μL DTPA (5.3×10^{-5} mol/L in 0.5 mol/L sodium citrate, pH 4.0) were mixed and incubated at room temperature for 60 min. ^{111}In-DTPA and In-DTPA were mixed shortly before use to achieve the desired specific activity.

[111]In-diDTPA was prepared from a tetrapeptide (Ac-Phe-Lys-Tyr-Lys) that was synthesized as described previously (1). The ε-NH_2 groups of both lysine residues of the peptide were substituted with DTPA. A kit containing 11 μg Ac-Phe-Lys(-DTPA)-Tyr-Lys(DTPA)-NH_2 (=diDTPA), 50 mg 2-hydroxypropyl-β-cyclodextrin, and 4.4 mg citrate (pH 4.2) was dissolved in 1 mL water. To 10 μL of this kit, 85 μL [111]$InCl_3$ (=31–62 MBq) were added and incubated for 10 min at room temperature. Labeling efficiency was determined using ITLC with 0.15 mol/L citrate, pH 6.0, as the mobile phase. As soon as labeling efficiency was >95%, a 2-fold molar excess of $InCl_3$ was added to saturate all DTPA moieties with In^{3+}. Analogously, Ac-Phe-Lys(-DTPA)-Tyr-Lys(DTPA)-NH_2 was loaded with nonradioactive $InCl_3$ and this preparation was added to the ^{111}In-labeled diDTPA to achieve the desired specific activity.

[99mTc]-diDTPA was prepared from the tetrapeptide Ac-Lys-Tyr-Lys-Lys. The ε-NH_2 groups of both lysine residues of the peptide were substituted with DTPA. The ε-NH_2 group of the C-terminal lysine residue was substituted with an N_2S_2 core (TscG-Cys-3-thiosemicarbazonylglyoxyl-cysteinyl) to allow labeling of the peptide with [99mTc] (9).

Scatchard Analysis

The affinity of the DTIn-1 antibody for ^{111}In-DTPA and for ^{111}In-diDTPA was determined in vitro. Ninety-six–well polystyrene plates (Costar, Cambridge, MA) were coated with rabbit antimouse antibodies (DAKO, Glostrup, Denmark) (1:1,000 in 0.1 mol/L Na_2CO_3, pH 9.6, 100 μL/well, 16 h at 4°C). Nonspecific binding sites were blocked by incubating the wells with phosphate-buffered saline (PBS), 0.5% BSA (200 μL/well, 1 h at 37°C). Subsequently, purified DTIn-1 antibody was added to the wells (20 μg/well, 100 μL/well, 1 h at 37°C). After washing (4 times with 200 μL PBS, 0.5% BSA), a serial dilution of ^{111}In-DTPA and of ^{111}In-diDTPA in PBS, 0.5% BSA (0.003–1 pmol, 10^3–10^6 cpm/well, 100 μL/well) was incubated in the wells (1 h at 37°C). After washing (4 times with 200 μL PBS, 0.5% BSA), the radioactivity in the wells (bound) was counted in a well-type scintillation γ-counter (Wizard 1430; Pharmacia, Uppsala, Sweden). A Scatchard plot (bound/free vs. bound) was made, and the K_a of the antibody for ^{111}In-DTPA and for ^{111}In-diDTPA was calculated from the slope of the plot.

Animal Studies

A *S. aureus* calf muscle abscess was induced in young, male Wistar rats (200–240 g body weight; Harlan, Horst, The Netherlands) as described previously (10). Experiments were initiated 24 h after the *S. aureus* inoculation. All radiopharmaceuticals were injected intravenously through the tail vein.

To determine the biodistribution of the radiolabel, rats were suffocated with CO_2. A blood sample was taken by cardiac puncture. Tissues were dissected and weighed. The activity in tissues and injection standards was measured in a shielded well-type scintillation γ-counter and expressed as the percentage of injected dose per gram (%ID/g). In all experiments, groups of 5 rats were used.

For scintigraphic imaging, groups of 3 rats were anesthetized (nitrous oxide, oxygen, and halothane) and placed prone on a gamma camera (Orbiter; Siemens, Hoffman Estates, IL) equipped with a medium-energy (^{111}In) or low-energy ([99mTc]) parallel-hole collimator. Images (300,000 counts per image) were obtained up to 2 h after injection and stored in a 256×256 matrix. All images were windowed identically, allowing a fair comparison among the various experiments.

In the first experiments, the most optimal radiolabeled hapten was selected. Three groups of 5 rats received 0.66 nmol (100 μg) anti-DTPA antibody intravenously. Four hours later, 0.3 nmol (20 μg) BSA-DTPA-In was injected, and 15 min thereafter, the rats received either ^{111}In-DTPA, ^{111}In-DTPA-Lys, or ^{111}In-diDTPA (8 pmol per rat, 4 MBq). After injection of the radioactivity, images were acquired at 5 min, 1 h, and 2 h as described above. After the last imaging session, the rats were killed and the biodistribution of the radiolabel was determined as described above. Next, the effect of the molecular weight of the blocking agent was investigated. Groups of 5 rats received 0.66 nmol (100 μg) anti-DTPA antibody intravenously. Four hours later, each group of rats received 0.3 nmol (20 μg) of the blocking agent (BSA-DTPA-In or IgM-DTPA-In), and 15 min thereafter, each group of rats received 4 MBq ^{111}In-diDTPA.

Subsequently, the dosing of the 3 agents (DTIn-1 antibody, BSA-DTPA-In, and ^{111}In-labeled diDTPA) and timing of the 3 injections were optimized in a series of imaging/biodistribution experiments in rats with *S. aureus* infection. In these experiments, the dose of the anti-DTPA antibody (0.67, 2, or 6 nmol per rat), the dose of the BSA-DTPA-In (0.3, 1, or 3 nmol per rat), and the dose of the ^{111}In-diDTPA (1.6, 8, or 40 pmol per rat) were varied. In addition, the timing of the 3 injections was optimized: the times between the first and the second injection (1, 4, and 24 h) and the time between the second and the third injection (5, 15, and 30 min) were varied.

Statistical Analysis

All mean values are presented as mean ± SD. Statistical analysis was performed using the nonparametric Mann–Whitney test, and the 2-tailed *P* was calculated.

RESULTS

Scatchard Analysis

The Scatchard plots of the in vitro assays for the binding of ^{111}In-DTPA and ^{111}In-diDTPA to the DTIn-1 antibody revealed that the affinity of DTIn-1 for bivalent ^{111}In-DTPA was 6 times higher than the affinity for monovalent ^{111}In-DTPA ($K_a = 0.87 \times 10^{-9}$ mol/L vs. 5.3×10^{-9} mol/L).

Optimization of 3-Step Approach

Structure of Radiolabeled Chelate. The structure of the radiolabeled chelate markedly affected the biodistribution of the radiolabel in the 3-step approach. As shown in Figure 1, the major fraction of the ^{111}In-DTPA injected in the third step was rapidly excreted to the urine of the rats and uptake of the radiolabel in the abscess was relatively low (0.08 ± 0.02 %ID/g 2 h after injection). Abscess uptake of ^{111}In-DTPA-Lys was similarly low (0.08 ± 0.01 %ID/g 2 h after injection), whereas there was considerable retention of the radiolabel in the kidneys (2.89 ± 0.35 %ID/g 2 h after injection) with this radiolabeled chelate. In contrast, when the bivalent chelate ^{111}In-diDTPA was injected in the third step, the uptake in the abscess was significantly higher (0.25 ± 0.04 %ID/g 2 h after injection, $P = 0.008$). Kidney retention with the bivalent chelate was similarly high, as with ^{111}In-DTPA-Lys (2.51 ± 0.22 %ID/g 2 h after injection). On the basis of these results, ^{111}In-diDTPA was used as the radiolabeled chelate in all further experiments.

Molecular Weight of Blocking Agent. We hypothesized that a blocking agent with a higher molecular weight would reduce the risk of blocking the anti-DTPA antibody activity in the infectious focus. Therefore, besides BSA-DTPA-In, a high-molecular-weight blocking agent was prepared using IgM as the carrier protein (relative molecular mass = 900,000 Da) with a similar DTPA substitution ratio (on a per-gram basis). The 3-step strategy was tested in 2 groups of rats with *S. aureus* infection, using either BSA-DTPA-In or IgM-DTPA-In in the second step. The molecular weight of the blocking agent did not significantly affect the biodistribution of the ^{111}In-diDTPA. When IgM-DTPA-In was used as the blocking agent, the blood levels of ^{111}In-diDTPA

were similar to those obtained with BSA-DTPA-In (0.41 ± 0.07 %ID/g vs. 0.41 ± 0.04 %ID/g, respectively, $P = 0.99$). Similarly, the uptake in the abscess obtained with each of the blocking agents was not significantly different (0.41 ± 0.05 %ID/g vs. 0.33 ± 0.06 %ID/g, respectively, $P = 0.06$). BSA-DTPA-In was chosen as the blocking agent in all further experiments.

Tuning of Dosing of 3-Step Strategy

Anti-DTPA Antibody Dose. The 3-step strategy was studied using 3 DTIn-1 antibody doses (0.67, 2, and 6 nmol/rat). In these experiments, the dose of the blocking agent was adjusted to the dose of the DTIn-1 antibody; in each group, a 3-fold molar excess blocking agent was administered, assuming that 45% of the injected DTIn-1 was in the blood compartment at 4 h after injection (blood level DTIn-1 at 2 h after injection, 2 %ID/g; blood volume, 12 mL). The dose of the DTIn-1 antibody did not have a marked effect on the uptake of the ^{111}In-diDTPA in the abscess or on the target-to-background ratios (data not shown); no significant differences in abscess uptake or in abscess-to-background ratios were observed. Highest abscess uptake (0.30 ± 0.07 %ID/g 2 h after injection) and abscess-to-contralateral muscle ratios (4.6 ± 1.1 two hours after injection) were obtained at the 2 nmol per rat (300 μg) DTIn-1 dose. Therefore, further experiments were conducted using a 2 nmol per rat DTIn-1 dose.

Dose of Blocking Agent. Using the fixed 2 nmol per rat DTIn-1 antibody dose, 3 doses of the BSA-DTPA-In blocking agent were tested in rats with *S. aureus* infection. Assuming that 45% of the injected DTIn-1 was still in the blood compartment at 4 h after injection, an equimolar amount (0.3 nmol per rat), a 3-fold molar excess (1 nmol per rat), and a 9-fold molar excess (3 nmol per rat) of BSA-DTPA-In were administered. The images acquired 2 h after injection of the ^{111}In-diDTPA indicated that the blocking agent dose of 1 nmol per rat was most optimal (Fig. 2). At this dose, the uptake in the abscess was 0.30 ± 0.08 %ID/g, whereas the activity levels in the blood were relatively low (0.32 ± 0.02 %ID/g). At the lower dose (0.3 nmol per rat),

chelate structure

DTPA   DTPA-Lys   diDTPA
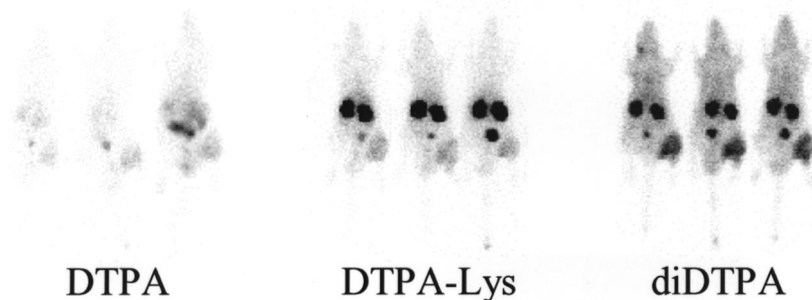
FIGURE 1. Scintigraphic images of rats with *S. aureus* calf muscle infections. Rats received 0.66 nmol (100 μg) anti-DTPA antibody intravenously. Four hours later, 0.3 nmol (20 μg) BSA-DTPA-In was injected as blocking agent, and 15 min thereafter, rats received ^{111}In-DTPA, ^{111}In-DTPA-Lys, or ^{111}In-diDTPA (8 pmol per rat, 4 MBq per rat). Images were acquired 2 h after injection of radiolabel.

blocking agent dose

0   0.3 nmole   1 nmole   3 nmole

FIGURE 2. Scintigraphic images of rats with *S. aureus* calf muscle infections. Rats received 300 µg (2 nmol) anti-DTPA antibody intravenously. Four hours later, each group of rats received BSA-DTPA-In (0–0.3, 1, and 3) to block anti-DTPA antibody activity in circulation. Fifteen minutes thereafter, rats received ^{111}In-diDTPA (8 pmol per rat, 4 MBq per rat). Images were acquired 2 h after injection of radiolabel.
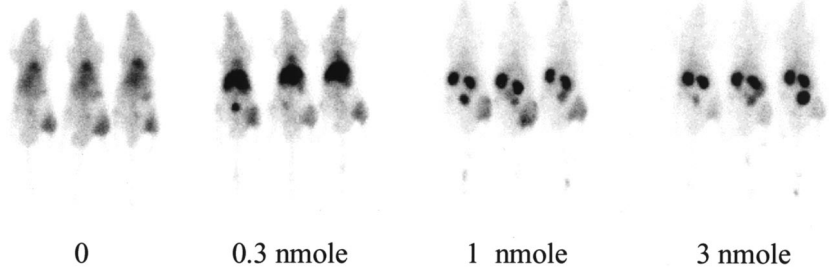
activity in the blood was significantly higher (0.89 ± 0.13 %ID/g, $P = 0.008$) and liver uptake was significantly enhanced (2.25 ± 0.47 %ID/g vs. 0.85 ± 0.28 %ID/g, $P = 0.008$), most likely because of hepatic clearance of high-molecular-weight DTIn-1 × ^{111}In-diDTPA immune complexes. At the higher BSA-DTPA-In dose (3 nmol per rat), uptake in the abscess was significantly decreased (0.21 ± 0.03 %ID/g, $P = 0.03$) (Fig. 2), presumably because of blockage of the DTIn-1 activity that localized in the infectious focus. Interestingly, when no blocking agent was administered, the 2-h postinjection image (Fig. 2A) of the biodistribution of the radiolabel resembled that of ^{111}In-IgG; clear visualization of the blood pool caused by high activity levels in the blood (3.01 ± 0.19 %ID/g), with relatively low uptake in the abscess (0.86 ± 0.35 %ID/g) and the kidneys (0.99 ± 0.21 %ID/g).

Dose of ^{111}In-diDTPA. Increasing amounts of diDTPA (1.6, 8, and 40 pmol per rat) labeled with identical amounts of ^{111}In (4 MBq per rat) were injected intravenously in the third step. As shown in Figure 3, optimal images were obtained at the 40-pmol dose. Ex vivo counting of the dissected tissues revealed that at this dose, abscess uptake was 0.30 ± 0.03 %ID/g, whereas the blood level was 0.20 ± 0.01 %ID/g. Although the uptake in the abscess was even higher at the 8-pmol dose level (0.38 ± 0.08 %ID/g, $P = 0.06$), the activity in the blood (0.47 ± 0.08 %ID/g) was 2.5-fold higher than at the 40-pmol dose level ($P =$

0.008). Consequently, uptake in all nontarget tissues was higher at the 8-pmol ^{111}In-diDTPA dose level. Remarkably, at the lowest ^{111}In-diDTPA dose (1.6-pmol per rat), the radiolabeled hapten rapidly cleared to the liver and spleen (liver uptake, 3.82 ± 0.24 %ID/g; spleen uptake, 1.95 ± 0.31 %ID/g; blood level, 0.17 ± 0.16 %ID/g). Apparently, the remaining DTIn-1 activity in the circulation formed high-molecular-weight immune complexes with the ^{111}In-diDTPA at this dose level. These immune complexes rapidly cleared to the liver and spleen.

Interval Between First and Second Injections. Three intervals between injection of the anti-DTPA antibody and injection of the blocking agent were tested: 1, 4, and 24 h. Optimal visualization of the infection was obtained with the 4-h interval (Fig. 4). Abscess uptake was optimal with the 4-h interval (0.39 ± 0.09 %ID/g) compared with the 1-h interval (0.29 ± 0.03 %ID/g, $P = 0.03$). No further improvement was observed when the interval was further extended to 24 h (abscess uptake, 0.35 ± 0.08 %ID/g, $P = 0.4$). Blood levels with each interval were similar (0.49 ± 0.05, 0.45 ± 0.03, and 0.51 ± 0.06 %ID/g, respectively).

Interval Between Second and Third Injections. The time span between injection of the blocking agent (BSA-DTPA-In) and injection of the radiotracer (^{111}In-diDTPA) (5–30 min) did not affect the in vivo distribution of the radiolabel (data not shown).

diDTPA dose

1.6 pmole   8 pmole   40 pmole

FIGURE 3. Scintigraphic images of rats with *S. aureus* calf muscle infections. Rats received 300 µg (2 nmol) anti-DTPA antibody intravenously. Four hours later, rats received 1 nmol BSA-DTPA-In as blocking agent. Fifteen minutes thereafter, each group of rats received ^{111}In-diDTPA (1.6, 8, and 40 pmol per rat, respectively; 4 MBq per rat). Images were acquired 2 h after injection of radiolabel.
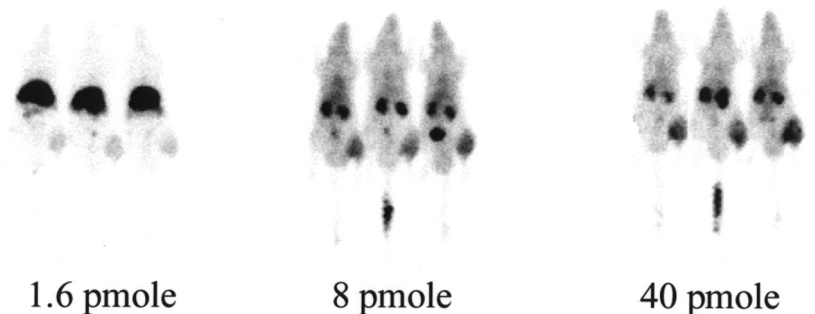
interval between 1st and 2nd injection

1 hr   4 hr   24 hr
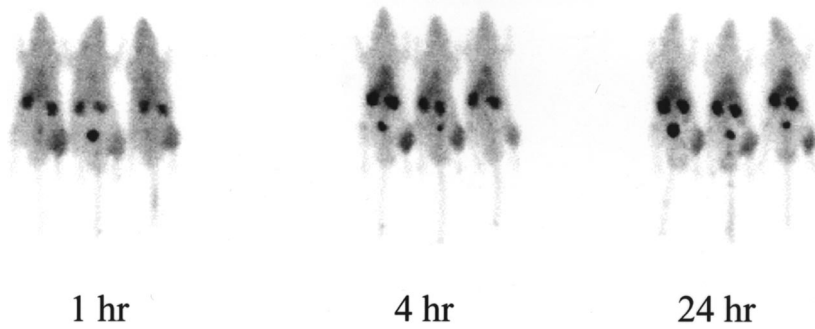
FIGURE 4. Scintigraphic images of rats with *S. aureus* calf muscle infections. Rats received 300 µg (2 nmol) anti-DTPA antibody intravenously. Rats received 1 nmol BSA-DTPA-In as blocking agent 1, 4, and 24 h later. Fifteen minutes thereafter, each group of rats received ^{111}In-diDTPA (8 pmol per rat, 4 MBq per rat). Images were acquired 2 h after injection of radiolabel.

Characterization of Optimized 3-Step Strategy

Comparison of 3-Step Approach with ^{111}In-IgG. The biodistribution of ^{111}In-diDTPA in the optimized 3-step approach (t = 0 h, 2 nmol DTIn-1 per rat; t = 4 h, 1 nmol BSA-DTPA-In per rat; t = 4 hr 5 min, 40 pmol ^{111}In-diDTPA per rat) was compared with that of ^{111}In-IgG (4 MBq per rat, 0.66 nmol [100 µg]). As shown in Figure 5, the biodistribution of the radiolabel in each group (5 h after injection of the DTIn-1 or the IgG) differed markedly. With the 3-step approach, virtually no activity accumulated in the liver (0.17 ± 0.02 %ID/g) and the blood (0.18 ± 0.01 %ID/g), whereas highest uptake was found in the kidneys (3.86 ± 0.70 %ID/g). In contrast, with ^{111}In-IgG, physiologic uptake was observed mainly in the liver (1.95 ± 0.28 %ID/g) and the blood (3.49 ± 0.30 %ID/g), whereas the kidneys (1.24 ± 0.14 %ID/g) were hardly visualized.

Application of ^{99m}Tc in 3-Step Approach. Substituting the ^{111}In-diDTPA bivalent chelate with the ^{99m}Tc-diDTPA-In compound (at optimized conditions: t = 0 h, 2 nmol DTIn-1 per rat; t = 4 h, 1 nmol BSA-DTPA-In per rat; t = 4 hr 5 min, 40 pmol ^{99m}Tc-diDTPA-In per rat) indicated that, despite the fact that the DTIn-1 antibody has a higher affinity for DTPA loaded with indium than with technetium, this 3-step approach can also exploit the favorable imaging characteristics of ^{99m}Tc (Fig. 6). The 2-h postinjection biodistribution data of the ^{99m}Tc label in the blood and the abscess were similar to those obtained with the ^{111}In-labeled bivalent chelate (Table 1, $P = 0.06$ and 0.3, respectively). Uptake of the ^{99m}Tc-diDTPA in the spleen, kidneys, and liver was significantly lower than that obtained with ^{111}In-diDTPA ($P = 0.008$, 0.02, and 0.008, respectively). These differences can be explained by the fact that ^{111}In-DTPA-Lys is completely retained in the lysosomes after it has been internalized, whereas chelated ^{99m}Tc is not (*11*).

DISCUSSION

In this study, we showed that infectious foci could be delineated relatively shortly after injection (≤6 h) with an

3-step with ^{111}In-diDTPA vs. ^{111}In-IgG

diDTPA   IgG-DTPA
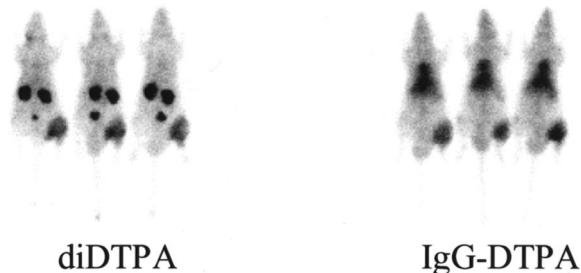
FIGURE 5. Scintigraphic images of rats with *S. aureus* calf muscle infections. One group of rats was imaged according to optimized 3-step approach (2 nmol anti-DTPA antibody; 4 h later, 1 nmol BSA-DTPA-In; 5 min later, 40 pmol ^{111}In-diDTPA). Other group of rats received ^{111}In-IgG (4 MBq, 0.66 nmol). Both groups of rats were imaged 5 h after first intravenous injection.

^{111}In-diDTPA vs. ^{99m}Tc-diDTPA

^{111}In-diDTPA ^{99m}Tc-diDTPA
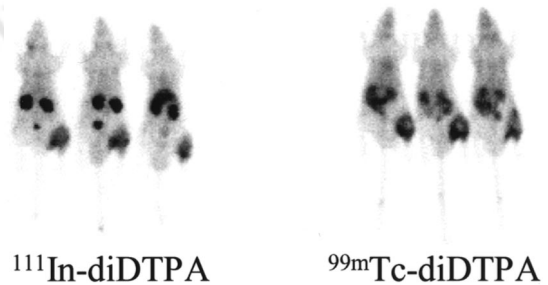
FIGURE 6. Scintigraphic images of rats with *S. aureus* calf muscle infections. Both groups received 2 nmol anti-DTPA antibody. Four hours later, anti-DTPA antibody activity in circulation was blocked with 1 nmol BSA-DTPA-In. Five minutes thereafter, one group of rats received 40 pmol ^{111}In-diDTPA (4 MBq), whereas other group received 40 pmol ^{99m}Tc-diDTPA (5 MBq). Images were acquired 2 h after injection of radiolabel.

TABLE 1
Biodistribution of Radiolabel (%ID/g) 2 Hours After Injection of Bivalent Radiolabeled Chelate

Tissue	^{111}In-diDTPA	^{99m}Tc-diDTPA
Blood	0.27 ± 0.03	0.23 ± 0.03
Muscle	0.04 ± 0.01	0.07 ± 0.02*
Abscess	0.34 ± 0.07	0.29 ± 0.13
Lung	0.25 ± 0.04	0.36 ± 0.02*
Spleen	0.40 ± 0.04	0.13 ± 0.03*
Kidney	2.56 ± 0.24	1.69 ± 0.16†
Liver	0.69 ± 0.03	0.22 ± 0.01*
Intestine	0.25 ± 0.05	0.22 ± 0.05

Two groups of rats ($n = 5$) received DTIn-1 (t = 0 h, 2 nmol per rat). BSA-DTPA-In (t = 4 h, 1 nmol per rat) and radiolabeled bivalent chelate (t = 4 hr 5 min, 40 pmol per rat) were injected. Radiolabel biodistribution was determined 2 h after injection of radiolabel.
*$P = 0.008$.
†$P = 0.02$.

antibody-based pretargeting strategy. There is a great need for an imaging technique that can localize infection accurately within a few hours, without the complex labeling procedures that apply for the preparation of radiolabeled autologous leukocytes. Using radiopharmaceuticals such as ^{67}Ga-citrate, radiolabeled nonspecific IgG, and intact radiolabeled antigranulocyte antibodies, a relatively long time (≥24 h) is needed before a final diagnosis can be made [12]. With these agents, the images with the most diagnostic information are usually acquired beyond 16 h because of the slow accumulation of these agents in the target tissues and their slow clearance from the background. In mouse tumor models and in clinical studies, it has been shown that pretargeting can improve targeting of tumor lesions [4,5,13].

Ruscskowski et al. [14] were among the first to develop a pretargeting strategy to image infection. In mice with *Escherichia coli* infection, they showed that the infectious foci could be imaged by injection of streptavidin followed by radiolabeled biotin [14,15]. In a previous study, we showed the feasibility of pretargeted infection imaging based on the anti-DTPA antibody DTIn-1 [6]. In these studies, ^{99m}Tc-labeled DTPA was used as the radiotracer. The affinity of the DTIn-1 antibody is highly dependent on the metal that is chelated; DTIn-1 has the highest affinity for ^{111}In-DTPA. Furthermore, in a mouse tumor model using antitumor × anti-DTPA bispecific antibodies (G250 × DTIn-1), we showed that uptake of the radiolabel in the tumor was at least 10-fold higher when the bivalent chelate ^{111}In-diDTPA was used instead of monovalent ^{111}In-DTPA [1]. It was hypothesized that this improved targeting of the tumor was caused by the so-called affinity enhancement system [16]; at the tumor cell surface, the diDTPA can be bound by anti-DTPA antibodies, resulting in more avid binding of the radiolabeled hapten. Here, we showed that the improved uptake and retention of the radiolabel can also be found when the anti-DTPA activity in the target is not cell bound. Our results are in line with those described by Goodwin et al. [17]. In a mouse tumor model, they showed that when the tumor was pretargeted nonspecifically with a monoclonal antichelate antibody, tumor uptake increased 2.6-fold when a bivalent chelate was used instead of a monovalent chelate.

As in previous pretargeting studies [1,6,17], this study showed that the dose of the agents involved, especially the blocking agent and the radiolabeled chelate, was also critical. The most striking effect was observed when the dose of the radiolabeled chelate ^{111}In-diDTPA was varied. Optimal targeting to the infectious focus without any hepatic accumulation was obtained at the 40-pmol dose, whereas virtually all the radioactivity rapidly cleared to the liver at the 1.6-pmol dose. The findings from our pretargeting studies with bispecific antibodies and ^{111}In-diDTPA in the nude mouse tumor model could not be extrapolated to the current rat model, because the mouse maximum uptake of the ^{111}In-diDTPA in the target was obtained at a very low ^{111}In-diDTPA dose (maximum specific activity) [1]. This paradox might be explained by the fact that the mouse tumor is a saturable target, whereas the infectious focus in the rat is practically unsaturable.

The use of a blocking agent was indispensable in this approach to prevent the formation of DTIn-1 × diDTPA immune complexes in the circulation. In fact, when the blocking agent was omitted, the pharmacokinetics of the radiolabeled chelate resembled those of a radiolabeled antibody. In most pretargeting strategies, a blocking or clearing agent is used to block or remove the pretargeting agent from the circulation [18–20]. In the mouse tumor model using G250 × DTIn-1 bispecific antibodies as a pretargeting agent, such a blocking agent was not required [1]. Apparently, the DTIn-1 × diDTPA immune complexes in the current approach were much more stable in serum than the monovalent complexes between the DTIn-1–based bispecific antibody and ^{111}In-diDTPA.

This 3-step targeting approach could improve imaging of infection and inflammation in patients because optimal images can be acquired 1–2 h after injection of the radiolabel (5–6 h after the first injection with the DTIn-1 antibody). A limitation of this approach might be the development of human antimouse antibodies after administration of DTIn-1. For clinical studies, a humanized DTIn-1 antibody would be preferable. Immunogenicity of the background-reducing agent can be minimized by the use of a human serum protein (e.g., human serum albumin) as a carrier. Alternatively, a nonimmunogenic synthetic blocking agent can be used, as has been developed by Theodore et al. [21]. In contrast to pretargeting strategies that exploit the avid interaction between biotin and streptavidin, the current pretargeting approach can be based on nonimmunogenic reagents [22]. Besides this 3-step approach, a series of new agents (e.g., chemotactic peptides, interleukins, antimicrobial peptides, and ciprofloxacin) has been developed for scintigraphic visualization of infection and inflammation

(*23*). Which of these agents ultimately will be applied clinically will be determined in future studies in patients.

CONCLUSION

With this 3-step pretargeting strategy, infectious foci can be rapidly imaged with low background levels. Clinical studies with a humanized anti-DTPA antibody and a non-immunogenic blocking agent are warranted to assess the potential of this approach in the clinic.

ACKNOWLEDGMENTS

REFERENCES

1. Boerman OC, Kranenborg MH, Oosterwijk E, et al. Pretargeting of renal cell carcinoma: improved tumor targeting with a bivalent chelate. *Cancer Res.* 1999; 59:4400–4405.
2. Knox SJ, Goris ML, Tempero M, et al. Phase II trial of yttrium-90-DOTA-biotin pretargeted by NR-LU-10 antibody/streptavidin in patients with metastatic colon cancer. *Clin Cancer Res.* 2000;6:406–414.
3. Weiden PL, Breitz HB, Press O, et al. Pretargeted radioimmunotherapy (PRIT) for treatment of non-Hodgkin's lymphoma (NHL): initial phase I/II study results. *Cancer Biother Radiopharm.* 2000;15:15–29.
4. Vuillez JP, Kraeber-Bodere F, Moro D, et al. Radioimmunotherapy of small cell lung carcinoma with the two-step method using a bispecific anti-carcinoembryonic antigen/anti-diethylenetriaminepentaacetic acid (DTPA) antibody and iodine-131 Di-DTPA hapten: results of a phase I/II trial. *Clin Cancer Res.* 1999; 5(suppl):3259s-3267s.
5. Kraeber-Bodere F, Bardet S, Hoefnagel CA, et al. Radioimmunotherapy in medullary thyroid cancer using bispecific antibody and iodine ^{131}I-labeled bivalent hapten: preliminary results of a phase I/II clinical trial. *Clin Cancer Res.* 1999;5(suppl):3190s–3198s.
6. Kranenborg MH, Oyen WJ, Boerman OC, et al. Rapid imaging of experimental infection with technetium-99m-diethylenetriaminepenta-acetic after anti-DTPA monoclonal antibody priming. *J Nucl Med.* 1997;38:901–906.
7. Kranenborg MH, Boerman OC, Oosterwijk-Wakka JC, de Weijert MCA, Corstens FHM, Oosterwijk E. Development and characterization of anti-renal-cell carcinoma x anti-DTPA bispecific monoclonal antibodies for two-phase targeting of renal-cell carcinoma. *Cancer Res.* 1995;55(suppl):5864s–5867s.
8. Hnatowich DJ, Childs RL, Lanteigne D, Najafi A. The preparation of DTPA-coupled antibodies radiolabeled with metallic radionuclides: an improved method. *J Immunol Methods.* 1983;65:147–157.
9. Karacay H, McBride WJ, Griffiths GL, et al. Experimental pretargeting studies of cancer with a humanized anti-CEA x murine anti-[In-DTPA] bispecific antibody construct and a [99m]Tc-/[188]Re-labeled peptide. *Bioconjug Chem.* 2000;11:842–854.
10. Oyen WJ, Claessens RA, van der Meer JW, Corstens FH. Biodistribution and kinetics of radiolabeled proteins in rats with focal infection. *J Nucl Med.* 1992; 33:388–394.
11. Duncan JR, Welch MJ. Intracellular metabolism of indium-111-DTPA-labeled receptor proteins. *J Nucl Med.* 1993;34:1728–1738.
12. Oyen WJ, Claessens RA, van der Meer JW, Rubin RH, Strauss HW, Corstens FH. Indium-111-labeled human nonspecific immunoglobulin G: a new radiopharmaceutical for imaging infectious and inflammatory foci. *Clin Infect Dis.* 1992;14: 1110–1118.
13. Barbet J, Kraeber-Bodere F, Vuillez JP, Gautherot E, Rouvier E, Chatal JF. Pretargeting with the affinity enhancement system for radioimmunotherapy. *Cancer Biother Radiopharm.* 1999;14:153–166.
14. Rusckowski M, Fritz B, Hnatowich DJ. Localization of infection using streptavidin and biotin: an alternative to nonspecific polyclonal immunoglobulin. *J Nucl Med.* 1992;33:1810–1815.
15. Hnatowich DJ, Fritz B, Virzi F, Mardirossian G, Rusckowski M. Improved tumor localization with (strept)avidin and labeled biotin as a substitute for antibody. *Nucl Med Biol.* 1993;20:189–195.
16. Le Doussal JM, Martin M, Gautherot E, Delaage M, Barbet J. In vitro and in vivo targeting of radiolabeled monovalent and divalent haptens with dual specificity monoclonal antibody conjugates: enhanced divalent hapten affinity for cell-bound antibody conjugate. *J Nucl Med.* 1989;30:1358–1366.
17. Goodwin DA, Meares CF, McCall MJ, McTigue M, Chaovapong W. Pre-targeted immunoscintigraphy of murine tumors with indium-111-labeled bifunctional haptens. *J Nucl Med.* 1988;29:226–234.
18. Le Doussal JM, Gruaz-Guyon A, Martin M, et al. Targeting of indium-labeled bivalent hapten to human melanoma mediated bispecific monoclonal antibody conjugates: imaging of tumors hosted in nude mice. *Cancer Res.* 1990;50:3445–3452.
19. Breitz HB, Weiden PL, Beaumier PL, et al. Clinical optimization of pretargeted radioimmunotherapy with antibody-streptavidin conjugate and ^{90}Y-DOTA-biotin. *J Nucl Med.* 2000;41:131–140.
20. Paganelli G, Grana C, Chinol M, et al. Antibody-guided three-step therapy for high grade glioma with yttrium-90 biotin. *Eur J Nucl Med.* 1999;26:348–357.
21. Theodore LJ, Axworthy B, Reno JM, inventors; NeoRx Corp., assignee. Hepatic-directed compounds and reagents for preparation thereof. U.S. patent 5,886,143. March 23, 1999.
22. Chinol M, Casalini P, Maggiolo M, et al. Biochemical modifications of avidin improve pharmacokinetics and biodistribution, and reduce immunogenicity. *Br J Cancer.* 1998;78:189–197.
23. Rennen HJ, Boerman OC, Oyen WJ, Corstens FH. Imaging infection/inflammation in the new millennium. *Eur J Nucl Med.* 2001;28:241–252.